

## Relationships between Luminescent Properties and Structure in $\beta$ -K<sub>2</sub>SO<sub>4</sub>-Type Orthophosphates

C. PARENT, M. BEN AMARA, P. BOCHU, G. LE FLEM,  
AND P. HAGENMULLER

*Laboratoire de Chimie du Solide du CNRS, Université de Bordeaux I, 351,  
cours de la Libération, 33405 Talence Cedex, France*

Received July 29, 1983; in revised form January 3, 1984

The conditions of a Ce<sup>3+</sup> → Tb<sup>3+</sup> energy transfer have been analyzed in the Na<sub>2+*x*</sub>Ca<sub>2(1-*x*)</sub>Ce<sub>*x*</sub>Tb<sub>*y*</sub>(PO<sub>4</sub>)<sub>2</sub> orthophosphates. Terbium green emission through uv cerium excitation is characterized by a very low yield. This result is the consequence of a sodium-rare-earth short range ordering even at low rare-earth concentrations and of lack of rigidity in the anionic sublattice.

### Introduction

Phosphors showing Ce<sup>3+</sup> → Tb<sup>3+</sup> energy transfer may be used industrially as green components in low pressure mercury vapor lamps. According to Dexter's theory (1) the efficiency of such a transfer is mainly related to overlapping between Ce<sup>3+</sup> emission and Tb<sup>3+</sup> excitation spectra.

The conditions of this overlapping have been previously investigated for a group of alkali orthophosphates and the influence of various parameters such as alkali content and alkali electropositivity has been examined (2).

In this publication, the correlation between rare-earth distribution within the cationic sublattice of orthophosphates and Ce<sup>3+</sup> → Tb<sup>3+</sup> energy transfer probability will be emphasized. The investigated materials are the orthophosphates with  $\beta$ -K<sub>2</sub>SO<sub>4</sub>-type structure belonging to the NaCaPO<sub>4</sub>-Na<sub>3</sub>Ln(PO<sub>4</sub>)<sub>2</sub> (Ln = Ce, Tb) systems. Their general formulas are Na<sub>2+*x*</sub>Ca<sub>2(1-*x*)</sub>Ln<sub>*x*</sub>(PO<sub>4</sub>)<sub>2</sub> (0 ≤ *x* ≤ 1) with a 2Ca<sup>2+</sup> = Na<sup>+</sup> + Ln<sup>3+</sup> coupled substitution.

### I. Preparation

The powder samples have been prepared from stoichiometric mixtures of sodium and calcium carbonate (Merck 99.5%), rare-earth oxides (CeO<sub>2</sub> and Tb<sub>4</sub>O<sub>7</sub> of Rhône-Poulenc 99.99% purity) and diammonium hydrogenophosphate (NH<sub>4</sub>)<sub>2</sub>HPO<sub>4</sub> (99%).

Three heat treatments with intermediate grindings were necessary to complete the reaction: 4 hr at 400°C and 15 hr at 950°C in an argon stream; in order to avoid the formation of tetravalent Ce<sup>4+</sup> and Tb<sup>4+</sup> ions a third annealing at 850°C was carried out in the presence of a slight excess of Na<sub>3</sub>PO<sub>4</sub> under argon-hydrogen (1%) atmosphere.

### II. Crystallographic Study

X-Ray powder diffraction reveals the existence of three domains in both Na<sub>2+*x*</sub>Ca<sub>2(1-*x*)</sub>Ln<sub>*x*</sub>(PO<sub>4</sub>)<sub>2</sub> systems (Ln = Ce, Tb).

NaCaPO<sub>4</sub> (*x* = 0) has been studied previously in detail (3). In the 0 < *x* ≤ 0.30 range the phases are isotypic with  $\beta$ -K<sub>2</sub>SO<sub>4</sub>.

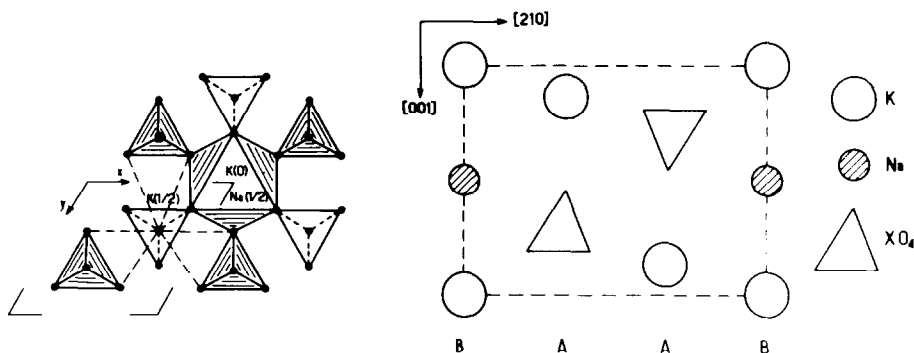


FIG. 1. Idealized structure of the  $K_3Na(SO_4)_2$  glaserite-type structure.

However, the superstructure lines which appear for  $NaCaPO_4$  vanish already for very low rare-earth contents. When  $0.30 < x \leq 1$  the X-ray pattern is similar to that of  $Na_3Nd(PO_4)_2$  (4) in the cerium system and to that of  $Na_3Nd(VO_4)_2$  (5) in the terbium one, both structures involving several different rare-earth sites.

The structure of all these compounds may be considered as deriving from the glaserite-type  $K_3Na(SO_4)_2$ , in which rows of  $|SO_4|$  tetrahedra and K atoms (A) alternate with rows of Na and K atoms (B), running along the  $\bar{c}$  axis of the hexagonal cell (Fig. 1).

Table I provides the obtained crystallographic data.

As has previously been established for similar system the  $|PO_4|$  groups and a part of the sodium atoms are located in the A rows. In the B sublattice three different arrangements have been found:

(i) In the starting phase  $NaCaPO_4$  ( $x = 0$ ) the B sites are all filled by calcium atoms.

(ii) When  $0 < x \leq 0.30$  there seems to be a random substitution of  $Na^+$  and  $Ln^{3+}$  for 2 neighboring  $Ca^{2+}$  ions as only long range ordering can be detected by X-ray diffraction.

(iii) When  $0.30 < x \leq 1$  the sodium and rare-earth rates become sufficient to induce an ordered distribution in the B rows. A 1-1 Na-Ln ordering appears within the B

sites for the  $Na_3Ce(PO_4)_2$  and  $Na_3Tb(PO_4)_2$  limit-compounds.

The luminescent properties have been studied only for materials with low rare-earth content ( $0 < x \leq 0.30$ ), in which  $Ce^{3+}$  and  $Tb^{3+}$  are located on a single site. This requirement is a condition for a theoretical transfer mechanism study.

### III. Optical Properties

#### III-1. Optical Properties of the $Na_{2+x}Ca_{2(1-x)}Ce_x(PO_4)_2$ phase ( $0 < x \leq 0.30$ )

As an example, Fig. 2 shows the  $Ce^{3+}$  emission ( $\lambda_{\text{ext.}} = 254 \text{ nm}$ ) and excitation ( $\lambda_{\text{em.}} = 400 \text{ nm}$ ) spectra of  $Na_{2.04}Ca_{1.92}Ce_{0.04}(PO_4)_2$ . The two large emission bands correspond to  $5d \rightarrow {}^2F_{7/2}$  and  $5d \rightarrow {}^2F_{5/2}$  transitions. The spectral overlapping of the excitation and emission bands is small, which indicates a large Stokes shift probably due to the rotational mobility of the  $|PO_4|$  groups (2, 7) and as a consequence to the lack of rigidity of the anionic network.

The cerium excited states lifetimes have been obtained by recording the cerium emission decay at 400 nm under a pulsed nitrogen laser excitation at 337.1 nm. The  $5d-4f$  transitions are parity and spin-allowed, and the shortness of such lifetimes

TABLE I  
CRYSTALLOGRAPHIC DATA OF THE  $K_3Na(SO_4)_2$  GLASERITE AND GLASERITE-RELATED  
ORTHOPHOSPHATES

Compounds	Parameters	Space group	Number of different rare-earth sites
$K_3Na(SO_4)_2$	$a_0$ $c_0$	$P\bar{3}m1$	—
$(NaCaPO_4)_2$ (3)	$a = 20.397 \text{ \AA} \approx 3c_0$ $b = 5.412 \text{ \AA} \approx a_0$ $c = 9.161 \text{ \AA} \approx a_0\sqrt{3}$	$Pn2_1a$	—
$Na_{2.30}Ca_{1.40}Ce_{0.30}(PO_4)_2$	$a = 7.015 \text{ \AA} \approx c_0$ $b = 5.342 \text{ \AA} \approx a_0$ $c = 9.253 \text{ \AA} \approx a_0\sqrt{3}$	$Pnma$ or $Pn2_1a$	1
$Na_3Ce(PO_4)_2$ (4)	$a = 16.08 \text{ \AA} \approx 3a_0$ $b = 14.14 \text{ \AA} \approx 2c_0$ $c = 18.72 \text{ \AA} \approx 2a_0\sqrt{3}$	$Pbc2_1$	6
$Na_{2.30}Ca_{1.40}Tb_{0.30}(PO_4)_2$	$a = 6.788 \text{ \AA} \approx c_0$ $b = 5.404 \text{ \AA} \approx a_0$ $c = 9.195 \text{ \AA} \approx a_0\sqrt{3}$	$Pnma$ or $Pn2_1a$	1
$Na_3Tb(PO_4)_2$ (5)	$a = 27.58 \text{ \AA} \approx 3a_0\sqrt{3}$ $b = 5.33 \text{ \AA} \approx a_0$ $c = 13.92 \text{ \AA} \approx 2c_0$ $\beta = 91.2^\circ$	$Cc$	3

required the use of a fast photomultiplier RTC 56 DUVP connected to a PHILIPS 3400 sampling oscilloscope and an  $X-Y$  recorder.

The method for the determination of lifetimes takes into account the rise time of the

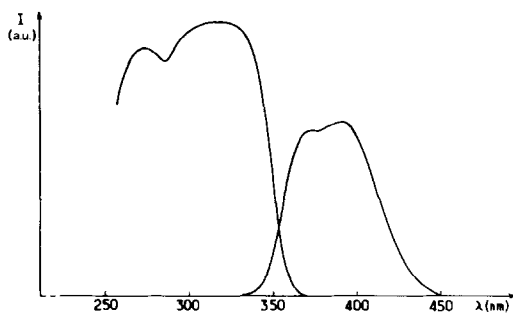


FIG. 2. Cerium emission (under 254-nm excitation) and excitation ( $\lambda_{em.} = 400 \text{ nm}$ ) spectra for  $Na_{2.04}Ca_{1.92}Ce_{0.04}(PO_4)_2$  at  $T = 300 \text{ K}$ .

experimental function (about 25 nsec). After 30 nsec, the decay function can be assumed to be exponential:  $I = I_0 \exp(-t/\tau_d)$ .

The  $\tau_d$  was found to be a constant:  $32 \pm 0.7 \text{ nsec}$  over the whole range of composition. The corresponding emission quantum yield has been calculated from absorption and emission intensities. It was found to be independent of cerium concentration (Fig. 3).

From another point of view  $\tau_d$  for  $Ce^{3+}$  ions in  $Na_{2.20}Ca_{1.60}Ce_{0.20}(PO_4)_2$  remains constant between 80 and 300 K.

All these results characterize a non-concentration quenching behavior due to the absence of energy-trapping defects. Such a situation is completely different from that observed for the  $KCaLa_{1-x}Ce_x(PO_4)_2$  phase, in which the existence of large tunnels in the lattice induces non-stoichiome-

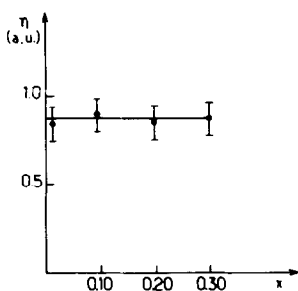


FIG. 3. Cerium emission quantum yield at  $T = 300$  K obtained with various  $\text{Na}_{2+x}\text{Ca}_{2(1-x)}\text{Ce}_x(\text{PO}_4)_2$  compounds under 254-nm excitation.

try with formation of  $\text{Ce}^{4+}$  energy absorbing defects (7).

### III-2. Existence of $\text{Ce}^{3+} \rightarrow \text{Tb}^{3+}$ energy transfer in $\text{Na}_{2+x+y}\text{Ca}_{2(1-x-y)}\text{Ce}_x\text{Tb}_y(\text{PO}_4)_2$

Three compositions were selected, corresponding to a low terbium content ( $y = 0.04$ ), and to an increasing proportion of  $\text{Ce}^{3+}$  ( $x = 0, 0.04, 0.20$ ).

Figure 4 exhibits the  $\text{Tb}^{3+}$  emission spectrum for the pure  $\text{Tb}^{3+}$  compound ( $x = 0, y = 0.04$ ) under 365-nm excitation at 300 K. The usual  $^5D_4 \rightarrow ^7F_J$  transitions were observed, among which the  $^5D_4 \rightarrow ^7F_5$  green component has the highest intensity.

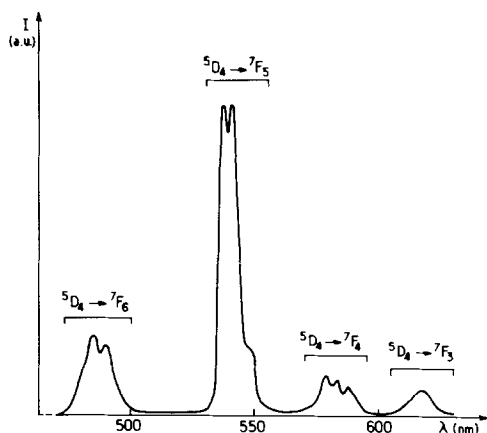


FIG. 4. Terbium  $^5D_4 \rightarrow ^7F_J$  ( $J = 3, 4, 5, 6$ ) emission under 365-nm excitation at  $T = 300$  K for  $\text{Na}_{2.04}\text{Ca}_{1.92}\text{Tb}_{0.04}(\text{PO}_4)_2$ .

Figure 5 shows the occurrence of a  $\text{Ce}^{3+} \rightarrow \text{Tb}^{3+}$  transfer in  $\text{Na}_{2.08}\text{Ca}_{1.84}\text{Ce}_{0.04}\text{Tb}_{0.04}(\text{PO}_4)_2$ ; the large excitation band found below 360 nm corresponds to the  $\text{Ce}^{3+}$  excitation band existing in the pure  $\text{Ce}^{3+}$  compound (Fig. 2).

Therefore, the  $\text{Ce}^{3+}$  lifetimes could be expected to decrease by introduction of  $\text{Tb}^{3+}$  in the crystal. In fact, it was found to be nearly constant for all compositions ( $\tau_d \approx 32$  nsec). Such a result means that the transfer quantum yield is very small.

Under these conditions, the experimental transfer quantum yield ( $\eta_T$ ) could be only estimated from cerium emission intensity in samples containing a donor alone ( $I_{d_0}$ ), or both donor and acceptor ( $I_d$ ) with the same donor concentration and under the same 254-nm excitation. Using the formula:  $\eta_T = 1 - I_{d_0}/I_d$ ,  $\eta_T$  was found to be  $\approx 0.05$  for all cerium concentrations.

### III-3. Theoretical Estimation of the $\text{Ce}^{3+} \rightarrow \text{Tb}^{3+}$ Direct Transfer Probability in $\text{Na}_{2.08}\text{Ca}_{1.84}\text{Ce}_{0.04}\text{Tb}_{0.04}(\text{PO}_4)_2$

Energy transfer from one center to another may occur via radiative transfer (i), exchange interaction (ii), and electric multipole-multipole interaction (iii) (1).

(i) Must be excluded due to the high value of the diffuse reflectance coefficient

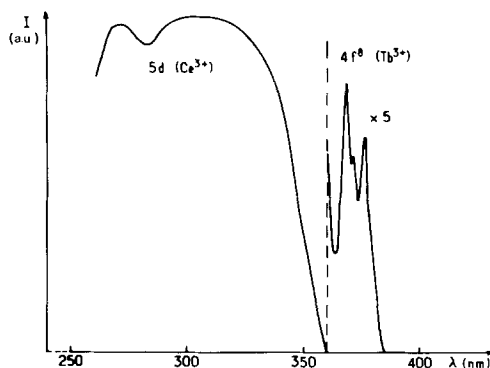


FIG. 5. Terbium excitation spectrum in  $\text{Na}_{2.08}\text{Ca}_{1.84}\text{Ce}_{0.04}\text{Tb}_{0.04}(\text{PO}_4)_2$ , for the  $^5D_4 \rightarrow ^7F_5$  emission at  $T = 300$  K.

(0.78) for the pure terbium phase in the cerium emission wavelength range.

(ii) The hypothesis of an exchange interaction can also be rejected. This type of transfer requires large direct or indirect overlap between donor and acceptor orbitals, leading to an easy electronic exchange.  $\text{Ce}^{3+}$  and  $\text{Tb}^{3+}$  are both strongly reducing ions and such an exchange would require too high an energy.

(iii) Multipolar interaction appears thus to be the most probable mechanism involved in the investigated phosphates. Cerium emission corresponds to an allowed electric dipolar radiation. Terbium  $4f \rightarrow 4f$  dipolar transitions are theoretically forbidden; consequently, the quadrupolar character of the  $\text{Tb}^{3+}$  transitions has to be taken into account. Therefore, both dipole-dipole ( $d-d$ ) and dipole-quadrupole ( $d-q$ ) mechanisms can be involved in the transfer.

As pointed out by Dexter (1) the corresponding probabilities  $P_{d-d}$  and  $P_{d-q}$  are proportional to  $R^{-6}$  and  $R^{-8}$ , respectively, where  $R$  is the donor-acceptor distance. Recent studies have shown that the  $P_{d-d}/P_{d-q}$  ratio is very high for low active ion concentrations and decreases at higher concentrations (8, 9).

All phosphates studied have a low  $\text{Tb}^{3+}$  content; thus, it was assumed for purposes of discussion that the electric dipole-dipole interaction was the predominant mechanism.

According to Dexter, the  $\text{Ce}^{3+} \rightarrow \text{Tb}^{3+}$  transfer probability  $P_{da}$  is given by the formula:

$$P_{da} = 0.63 \times 10^{28} \frac{Q_a}{R^6} \frac{1}{\tau_{d_0}} \int \frac{f_d(E) F_a(E)}{E^4} dE \quad (1)$$

in which

— $\tau_{d_0}$  is the radiative lifetime of the donor ( $\approx 32$  nsec),

— $Q_a$  is the acceptor absorption cross section ( $30 \times 10^{-23} \text{ cm}^2 \text{ eV}$ ) (10, 11).

— $\int f_d(E) F_a(E) E^{-4} dE = I$  is the overlap integral between cerium emission ( $f_d(E)$  taken between 330 and 450 nm) and terbium excitation ( $F_a(E)$  between 290 and 390 nm) normalized spectra. It was evaluated by Simpson's method.

— $R$  takes into account only the active ions located within a sphere whose radius has the critical  $R_0$  value for which the energy transfer becomes more probable than the donor radiative emission ( $P_{da} > 1/\tau_{d_0}$ )

From Eq. (1), using  $P_{da} = 1/\tau_{d_0}$ , one obtains  $R_0 \approx 5 \text{ \AA}$ .

In the crystal structure of  $\text{Na}_{2.08}\text{Ca}_{1.84}\text{Ce}_{0.04}\text{Tb}_{0.04}(\text{PO}_4)_2$  the four  $Ln$  positions around a given  $\text{Ce}^{3+}$  ion within the distance  $R_0$  are located, respectively, at 3.50  $\text{\AA}$  in the same B row for the two nearest ones and at 4.57  $\text{\AA}$  in two neighboring B rows for the two others (3).

$P_{da}$  must be calculated for both cases by introducing the occupancy factor by  $\text{Tb}^{3+}$  for each B cationic site.

In the first model calculation, allowing the presence of  $\text{Tb}^{3+}$  as nearest neighbors to  $\text{Ce}^{3+}$  in the same B rows, one finds  $P_{da} = 12 \times 10^6 \text{ sec}^{-1}$ ; the calculated transfer quantum yield  $\eta_T = P_{da}/P_{da} + 1/\tau_{d_0} = 0.28$  then is very high.

In a second calculation, the two nearest  $\text{Tb}^{3+}$  ions are assumed to be located only in the neighboring B rows; now  $P_{da} = 2.4 \times 10^6 \text{ sec}$  and  $\eta_T = 0.07$ . This value is in much better agreement with the experimental one (0.05).

#### IV. Discussion

These results can be analyzed from both crystallographic (a) and optical (b) viewpoints.

(a) In the phases with  $\beta\text{-K}_2\text{SO}_4$ -type structure ( $0 < x \leq 0.3$ ) the coupled substitution  $2\text{Ca}^{2+} \rightarrow Ln^{3+} + \text{Na}^+$  may involve two  $Ln^{3+}$  nearest neighbors in different B rows.

But in the same B row two neighboring  $Ln^{3+}$  ions must be separated from each other at least by one intervening  $Na^+$  ion.

Such a cationic distribution, which results in a decreasing of the cationic repulsion, is in complete agreement with all the previous crystallographic data concerning the  $Na_3Ln(PO_4)_2$  orthophosphates. At low temperature they exhibit always a 1-1  $Ln$ - $Na$  ordering within the B sublattice (6).

Consequently, in the entire  $Na_{2+x}Ca_{2(1-x)}Ln_x(PO_4)_2$  system ( $0 < x \leq 1$ ), there is a continuity in the  $Na^+ - Ln^{3+}$  distribution: the long range ordering which tends to appear near  $x = 0.30$  corresponds to a type of percolation threshold.

(b) In such orthophosphates, the easy rotation of the  $[PO_4]$  groups provides a large Stokes shift; accordingly, the overlapping between  $Ce^{3+}$  emission and excitation spectra is weak (Fig. 2).

As a consequence, even for a higher  $Ce^{3+}$  content ( $x = 0.20$ ), there is no significant migration energy between those  $Ce^{3+}$  ions which would be able to increase the green emission yield.

In consonance with this assumption, if the entire  $Na_{2+x+y}Ca_{2(1-x-y)}Ce_xTb_y(PO_4)_2$  system is considered, as it has been previously shown, the optimization of the green emission is observed for the limiting phase  $Na_3Ce_{0.65}Tb_{0.35}(PO_4)_2$  (12), which contains a high proportion of both  $Ce^{3+}$  and  $Tb^{3+}$ . However, the occurrence of several different sites for the rare earths makes it impossible to provide a theoretical study of this phosphor.

This behavior must be compared with the results obtained for low Stokes shift materials, in which a high  $Ce^{3+} \rightarrow Ce^{3+}$  transfer probability increases the quantum efficiency of the  $Tb^{3+}$  emission even for a low cerium content (13).

## References

1. D. L. DEXTER, *J. Chem. Phys.* **21**, 836 (1953).
2. P. BOCHU, C. PARENT, A. DAOUDI, G. LE FLEM, AND P. HAGENMULLER, *Mater. Res. Bull.* **16**, 883 (1981).
3. M. BEN AMARA, M. VLASSE, G. LE FLEM, AND P. HAGENMULLER, *Acta Crystallogr.* **c39**, 1483 (1983).
4. R. SALMON, C. PARENT, M. VLASSE, AND G. LE FLEM, *Mater. Res. Bull.* **13**, 439 (1978).
5. C. PARENT, J. FAVA, R. SALMON, M. VLASSE, G. LE FLEM, P. HAGENMULLER, E. ANTIC-FIDANCEV, M. LEMAITRE-BLAISE, AND P. CARO, *Nouv. Chim.* **3** (8/9), 523 (1979).
6. M. VLASSE, C. PARENT, R. SALMON, G. LE FLEM, AND P. HAGENMULLER, *J. Solid State Chem.* **35**, 318 (1980).
7. C. PARENT, P. BOCHU, G. LE FLEM, AND P. HAGENMULLER, J. C. BOURCET, AND F. GAUME-MAHN, *J. Phys. Chem. Solids* **45**(1), 39 (1984).
8. R. K. WATTS, in "Optical Properties of Ions in Solids" (B. Di Bartollo, Ed.), Plenum, New York (1975).
9. B. MOINE, J. C. BOURCET, G. BOULON, R. REISFELD, AND Y. KALISKY, *J. Phys.* **42**, 499 (1981).
10. R. REISFELD, E. GREENBERG, R. VELAPOLDI, AND B. BARNETT, *J. Chem. Phys.* **56**, 1698 (1972).
11. V. T. CARNALL, P. P. FIELDS, AND K. RAJNAK, *J. Chem. Phys.* **49**, 4412 (1968).
12. C. PARENT, J. FAVA, R. SALMON, G. LE FLEM, AND P. HAGENMULLER, *Solid State Commun.* **35**(6), 451 (1980).
13. B. SAUBAT, C. FOUASSIER, P. HAGENMULLER, AND J. C. BOURCET, *Mater. Res. Bull.* **16**, 193 (1981).